Theory and Verification of a new 3D RANS Wake Model

Philip Bradstock[1] and Wolfgang Schlez[1]

[1]ProPlanEn Ltd, 71-75 Shelton Street, WC2H 9JQ London, United Kingdom

Correspondence: Wolfgang Schlez (wolfgang.schlez@proplanen.com)

Abstract. This paper details the background to the WakeBlaster model: a purpose built, parabolic three-dimensional RANS solver, developed by ProPlanEn. WakeBlaster is a field model, rather than a single turbine model; it therefore eliminates the need for an empirical wake superposition model. It belongs to a class of very fast (a few core seconds, per flow case) mid-fidelity models, which are designed for industrial application in wind farm design, operation and control.

5   The domain is a three-dimensional structured grid, with approximately 80 nodes covering the rotor disk, by default. Wake-Blaster uses eddy viscosity turbulence closure, which is parameterized by the local shear, time-lagged turbulence development, and stability corrections for ambient shear and turbulence decay. The model prescribes a profile at the end of the near-wake, and the spatial variation of ambient flow, by using output from an external flow model.

    The WakeBlaster model is verified, calibrated and validated using a large volume of data from multiple onshore and offshore
10   wind farms. This paper presents example simulations for one offshore wind farm.

1 Introduction

In wind farms, wind turbines located downstream of other turbines will experience wake losses. Wind farm development and assessment processes require multiple iterations of configurations, as well as fast project turnaround.

    A good understanding of how wake loss works can give a company the competitive edge, while an unexpected systematic
15   performance loss can eliminate the expected profit from a project, or even from an entire project pipeline. Given the importance of wake losses, it may appear contradictory that many in the industry still use analytical single turbine wake models based on an approach suggested 40 years ago by Lissaman (1979) and Lissaman et al. (1982), who transferred the work of Abramovich (1963) on free jets to wind turbine wakes. Jensen (1983) presented what is still the most prominent model in this category. Other prominent models of this type include numerical solutions by Ainslie (1988) and Ott (2011). More recent analytical
20   models include that of Ishihara and Qian (2018).

    The longevity of the single wake model approach also speaks for the quality and practical usefulness of these early models. However, in order to provide accuracy for the full range of wind farms (e.g. large wind farms, closely cross-spaced farms, low hub height wind farms, wind farms with stable conditions, or offshore wind farms), an increasing number of empirical corrections had to be made, and parameters added, informed by new experimental data from wind farms, scale experiments,
25   or higher fidelity models - see, for example, Liddell et al. (2005), Schlez et al. (2006), citetSchlez2009, and Beaucage et al. (2012). A range of analytical single wake models and superposition methods are reviewed by Porté-Agel et al. (2019).

The increased computational power and scalability available today allows higher fidelity wake models to be used in the iterative process of wind farm design. These models widen the operational envelope, include more physics, and reduce model uncertainties in non-standard situations. We present the theory behind one such model: a 3D RANS (Reynolds Averaged
30 Navier-Stokes) wind farm wake model, WakeBlaster.

1.1 Related Work

In order to gain a more detailed understanding of wake losses in a wind energy research context, two groups of 3D-RANS codes have been developed. The models are referred to as 'field models', to distinguish them from the single turbine models by Crespo et al. (1999).
35 The first group of 3D-RANS codes are parabolic solvers, using the thin shear layer approximation, see Ferziger et al. (1997). Crespo et al. developed UPMWAKE at UPM (Universidad Polytechnica de Madrid), and later Crespo et al. (1994) based a parabolic model of the flow field inside a wind farm, called UPMPARK, on it. A number of further variants have been developed and reviewed by Vermeer et al. (2003). One branch was continued by TNO/ECN (The Energy Research Center of the Netherlands), and it resulted in the WakeFarm presented by Schepers (2003), and FarmFlow model presented in Eecen
40 et al. (2011). Renewed interest in mid-fidelity models has recently led to the independent development of several new models in this group, like those presented by Trabucchi et al. (2017) and Martinez-Tossas (2019).

The second group of 3D-RANS field models, the elliptic solvers, is more widespread. Elliptic solvers are used across other industries to parabolic solvers, and they are generally more powerful, but computationally (by several orders of magnitude) more expensive. These models use a k-ϵ or k-ω turbulence closure, describing the generation and dissipation of turbulent kinetic
45 energy. Models of this group are, in principle, also capable of solving the upstream effects of wind turbines. Some models are based on general purpose flow solvers, whereas others are in-house developments - examples can be found in the publications by Crespo et al. (1988); Prospathopoulos et al. (2010); Barthelmie et al. (2011); Laan et al. (2017); Michelsen (1994).

The WakeBlaster model developed by ProPlanEn by Schlez et al. (2017) belongs to the parabolic solver group. A parabolic solution offers a good balance between improved accuracy, additional detail, and computational costs. The target of the new
50 model is to improve the accuracy of wind farm loss modelling. Two specific aims are to address the interaction between wakes, as well as the interaction between wakes and the atmospheric boundary layer for different levels of atmospheric stability. Special attention was paid to the validation of the model, using data from a wide range of wind farms and atmospheric conditions.

The fundamental equations and assumptions for this solver are shown in the following Section 2. Section 3 presents as example the verification of the model for an offshore wind farm and the results of verifying the computational performance.
55 Section 4 discusses model limitations, followed by the conclusions in Section 5.

2 Theory

The WakeBlaster wind farm simulator is based on a Reynolds-Averaged Navier-Stokes (RANS) set of equations, which is used to solve the propagation of wake dissipation through the farm domain, in Cartesian 3D coordinates. In order to account for the

60 unsteady terms, it uses eddy viscosity turbulence closure, where the eddy viscosity is calculated from the combined wake and ambient wind speed shear profiles.

2.1 RANS Equations

The wake model uses RANS equations for momentum conservation, and mass flow conservation to calculate the three components of wind velocity in the axial, lateral and vertical directions. We use Cartesian 3D vectors for displacement $\overrightarrow{\mathbf{x}}$ and wind speed relative to ambient $\overrightarrow{\mathbf{u}}$: $\overrightarrow{\mathbf{x}} = \begin{bmatrix} x, y, z \end{bmatrix}$ $\overrightarrow{\mathbf{u}} = \begin{bmatrix} u, v, w \end{bmatrix}$, where the first element of the vectors (x) is along the mean wind

65 direction, the second element (y) is horizontal and perpendicular to (x), and the third element (z) is vertical (starting from the ground up) and makes up a right-hand coordinate system.

The Reynolds averaged momentum and mass conservation equation can be expressed for an incompressible flow in two dimensions, as given by Abramovich (1963):

$$\frac{\partial u}{\partial t} + \frac{\partial u^2}{\partial x} + \frac{\partial \overline{u'u'}}{\partial x} + \frac{\partial (uv)}{\partial y} + \frac{\partial \overline{u'v'}}{\partial y} = \mu \frac{\partial^2 u}{\partial y^2} + -\frac{1}{\rho}\frac{\partial p}{\partial x} \tag{1}$$

70 where u', v' and w' denote fluctuations from mean values.

2.2 Simplifying Assumptions

The following assumptions are applied for a stationary free wake, expanding into an infinite region:

Viscosity The effect of viscosity is small $\mu \frac{\partial^2 u}{\partial y^2} = 0$

Pressure Flow pressure gradients can be neglected $\frac{1}{\rho}\frac{\partial p}{\partial x}$

75 **Stationary** $\frac{\partial u}{\partial t} = 0$

Thin shear layer approximation $\frac{\partial \overline{u'u'}}{\partial x} = 0$

After substituting the continuity equation Abramovich (1963) obtains:

$$u\frac{\partial u}{\partial x} + v\frac{\partial u}{\partial y} + \frac{\partial \overline{u'v'}}{\partial y} = 0 \tag{2}$$

or expanded to three dimensions:

80 $$u\frac{\partial u}{\partial x} + v\frac{\partial u}{\partial y} + w\frac{\partial u}{\partial z} + \frac{\partial \overline{u'v'}}{\partial y} + \frac{\partial \overline{u'w'}}{\partial z} = 0 \tag{3}$$

and using the eddy viscosity turbulence closure:

$$-\frac{\partial \overline{u'v'}}{\partial y} = \bar{\epsilon}\frac{\partial^2 u}{\partial y^2} \quad -\frac{\partial \overline{u'w'}}{\partial z} = \bar{\epsilon}\frac{\partial^2 u}{\partial z^2} \tag{4}$$

where $\bar{\epsilon}$ denotes the eddy viscosity, which is considered to be scalar and isotropic. This leads to the governing momentum conservation equation:

$$u\frac{\partial u}{\partial x} + v\frac{\partial u}{\partial y} + w\frac{\partial u}{\partial z} - \bar{\epsilon}\frac{\partial^2 u}{\partial y^2} - \bar{\epsilon}\frac{\partial^2 u}{\partial z^2} = 0 \qquad (5)$$

while maintaining continuity:

$$\frac{\partial u}{\partial x} + \frac{\partial v}{\partial y} + \frac{\partial w}{\partial z} = 0 \qquad (6)$$

2.3 Numerical Solution

The ambient wind field is determined by an external flow model, and it determines the inflow conditions and spatial variations over a site. The turbine is represented by its hub height, diameter and other readily available and measured characteristics.

2.3.1 Wind Turbine Momentum Extraction

The waked wind field is set up by creating a two-dimensional flow plane, which forms a cross-section along the y and z axes of the velocity vector $\overline{u}$. The flow plane is bounded by the ground, at $z = 0$, and is large enough above and to the side of the resident wind turbines to ensure that boundary conditions have no more than a negligible impact on wake dissipation. The flow plane is propagated downstream along the x coordinate and, at each point along the x coordinate when it passes a turbine, a wake is injected into the flow plane.

Axial-momentum theory prescribes pressure building up in the induction zone upstream of any wind turbine or wind farm, and pressure recovery in the near-wake downstream of the rotor. The momentum that each of the turbines extracts in the process is the wind speed dependent thrust coefficient, as a function of the idealised incident wind speed, U_{inc}, at each turbine location, without the presence of the turbine.

In the model, the momentum deficit is injected at the end of the near-wake, for each turbine, and it is distributed over an expanded rotor area, using the blunt bell-shaped wind speed deficit profile from Lissaman et al. (1982). The centre-line wind speed U_{cent}, experimentally determined by Ainslie (1988) is used as a function of inflow turbulence α and thrust coefficient c_t.

$$U_{cent} = U_{inc}(c_t - 0.05 - (16c_t - 0.5)\frac{\alpha}{10}) \qquad (7)$$

The radial width of the profile is then derived by ensuring momentum conservation with regard to the thrust coefficient of the turbine.

2.3.2 Flow Plane Propagation

The flow plane is propagated according to equation 5 using the alternating direction implicit (ADI) method described by Peaceman and Rachford (1955); von Rosenberg (1983), where it is alternately solved in the xy and xz planes, incrementing

the x (downstream) coordinate by half a propagation step between each solving plane, so that both planes are solved once per step. By solving for each row or column in the flow plane, and by employing the central difference method, the problem can be set up numerically in a tridiagonal matrix equation, which can then be solved efficiently for the axial velocity, u, by the Thomas algorithm Thomas (1949), described for example in Burden and Faires (2001). In 3D Cartesian coordinates the

115   tridiagonal equation must be solved for every row or column of the flow plane, depending on which direction we are solving for. Dirichlet boundary conditions are used by enforcing $u = 1$ in the extremities of the flow plane.

At each half-step of the solving process, the lateral and vertical velocities, v and w respectively, are calculated for all points in the flow plane according to 6. For any given step there are two unknowns in this equation, v and w, and therefore it cannot be solved analytically in a single step. Instead, the unknowns are calculated numerically, by calculating each individually, and

120   iterating until their values converge. By rearranging equation 6, v and w can be expressed individually for a parabolic flow:

$$v = -\int \frac{\partial u}{\partial x} + \frac{\partial w}{\partial z} dy \quad ; \quad w = -\int \frac{\partial u}{\partial x} + \frac{\partial v}{\partial y} dz \tag{8}$$

In practice, due to the assumption of incompressibility, this formulation will lead to a local velocity shear, resulting in non-zero lateral and vertical velocities that are infinitely far from the source of shear. In reality this would not be the case, due to the compressibility of air. Therefore, in order to account for the effect of compressibility, a spatial damping term is introduced,

125   so that v and w tend to zero at $y = -\infty$, $y = \infty$ and $z = \infty$:

$$v = -\int \left(\frac{\partial u}{\partial x} + \frac{\partial w}{\partial z} - \gamma v \right) dy \quad ; \quad w = -\int \left(\frac{\partial u}{\partial x} + \frac{\partial v}{\partial y} - \gamma w \right) dz \tag{9}$$

where γ is a user-configurable positive constant that determines the strength of lateral and vertical velocity damping. As these integrals are indefinite, boundary conditions must be assigned. In the vertical direction, it is a given that vertical velocity at ground level is zero, as mass flow cannot pass into or out of the ground. Therefore, the condition $w_{z=0} = 0$ is applied, leading

130   to:

$$w(z) = -\int_0^z \left(\frac{\partial u}{\partial x} + \frac{\partial v}{\partial y} - \gamma w \right) dz' \tag{10}$$

In the lateral direction, the physical boundary conditions are that $v_{y=-\infty} = v_{y=\infty} = 0$, because the wind farm wakes cannot induce lateral velocity far from the farm. However, for numerical purposes, the size of the flow plane is constrained, and it cannot be guaranteed that the velocity will reach zero on both sides of the flow plane. Therefore, the lateral velocity is

135   integrated in each direction, starting from zero, and the mean of the two is taken. This is expressed as:

$$v(y) = -\frac{1}{2} \int_{y_{min}}^{y} \left(\frac{\partial u}{\partial x} + \frac{\partial w}{\partial z} - \gamma v \right) dy' + \frac{1}{2} \int_{y_{max}}^{y} \left(\frac{\partial u}{\partial x} + \frac{\partial w}{\partial z} - \gamma v \right) dy' \tag{11}$$

where y_{min} and y_{max} are the lateral location of the edge of the flow plane.

2.4 Eddy Viscosity Calculation

The key term controlling the rate of wake dissipation is eddy viscosity. Eddy viscosity has dimensions of length squared over
140 time, and it can be represented by multiplying a length scale of the shear layer by a velocity scale of the flow field.

WakeBlaster calculates eddy viscosity from the shear profile of axial velocity in the yz plane. In order to do this, it creates a combined flow plane of the ambient wind speed, U_{amb}, multiplied by the solved wake flow plane, u, which is relative to ambient wind speed. In neutral atmospheric conditions, the ambient wind speed is calculated as a logarithmic function of height above ground:

$$145 \quad U_{amb}(z) = \frac{u^*}{\kappa} \ln \frac{z}{z_0} \tag{12}$$

where u^* is the friction velocity, taken to be 2.5 times the value of standard deviation of the axial wind velocity, κ is the von-Karman constant (value = 0.4) and z_0 is the roughness length. The unknown parameters are determined from inputs to the simulation, such as wind speed and turbulence intensity at a particular height (usually the hub height of one of the turbines). The eddy viscosity is then calculated for every point in the flow plane, using the following process:

150 1. Create a combined flow plane by multiplying the ambient surface layer wind speed profile by the waked flow plane velocity u.

2. For each point, identify the local minimum and maximum velocity. For a point located at (y, z), local is determined as the range $[y - \eta z, y + \eta z]$ and $[(1 - \eta)z, (1 + \eta)z]$, in the lateral and vertical directions respectively, where η is a configurable constant which meets the criterion $0 < \eta < 1$.

155 3. In each of the two directions, the component of eddy viscosity is calculated as $\epsilon_i = \Delta u_i \Lambda_i$, where Δu_i is the difference between minimum and maximum velocity and Λ_i is the distance between the maximum and minimum points. This process is shown in figure 1.

4. The overall scalar velocity is the calculated as $\bar{\epsilon} = k \sqrt{\epsilon_y^2 + \epsilon_z^2}$, where k is a configurable calibration constant.

For a logarithmic wind speed profile in the vertical direction with no lateral variation, this method leads to an eddy viscosity
160 that is proportional to the height above ground.

2.4.1 Eddy Viscosity Lag

The eddy viscosity, as so far described in section 2.4, is solely based the wind shear profile. However, no newly created shear profile instantly generates turbulence, and therefore eddy viscosity - in reality, there is a lag between the change in a shear profile and its effect upon eddy viscosity and wake dissipation. In WakeBlaster this lag is formulated in terms of downstream
165 distance, and it has two distinct models.
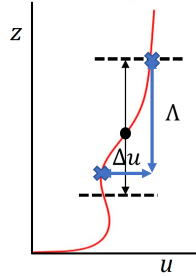
Figure 1. Calculation of the vertical component of eddy viscosity by finding the points of minimum and maximum velocity within a given height range.

The 'fixed' model obeys a first order lag equation:

$$\ell\Lambda\frac{d\epsilon}{dx} + \epsilon = \bar{\epsilon} \tag{13}$$

where ϵ is the lagged eddy viscosity, Λ is the length-scale defined in the previous section, and ℓ a configurable constant defining the lag length relative to the length scale.

170 The 'turbulence dependent' model gives a larger lag distance when the eddy viscosity and turbulence are low, and it obeys the following equation:

$$\frac{\Lambda}{\phi\frac{\epsilon}{kz} + \frac{\Lambda}{\lambda_{max}}}\frac{d\epsilon}{dx} + \epsilon = \bar{\epsilon} \tag{14}$$

where ϕ is a configurable parameter that determines the strength of turbulence on the lag length, and λ_{max} is also a configurable parameter that corresponds to the lag length when turbulence is zero.

175 **2.4.2 Atmospheric Stability**

When simulating atmospheric conditions that are not neutral, the calculation of eddy viscosity is modified. This modification uses the Monin-Obukhov length, L, and the concept of non-dimensional wind shear, ϕ_m, which is defined by Businger (1971), as:

$$\phi_m = \frac{\kappa z}{u*}\frac{\partial U}{\partial z} \tag{15}$$

180   Furthermore, according to Businger (1966), the non-dimensional wind shear is empirically approximated as what tends to be known as the Businger-Dyer relationship:

$$
\phi_m = \begin{cases} 1 + 5\zeta & \text{stable } (L > 0) \\ 1 & \text{neutral } (L \text{ undefined}) \\ (1 - 16\zeta)^{-\frac{1}{4}} & \text{unstable } (L < 0) \end{cases} \tag{16}
$$

where $\zeta = \frac{z}{L}$. The ambient wind speed shear profile is then modified by introducing ψ_m:

$$
U_{amb}(z) = \frac{u*}{\kappa} ln\left(\frac{z}{z_0} + \psi_m(\zeta)\right) \tag{17}
$$

185   where:

$$
\psi_m = \int_{\zeta_0}^{\zeta} [1 - \phi_m] d\zeta \tag{18}
$$

where $\zeta_0 = \frac{z_0}{L}$. Furthermore, the vertical component of the eddy viscosity, ϵ_z, is also modified by the non-dimensional wind shear:

$$
\epsilon_z = \frac{\Delta u_z \Lambda_z}{\phi_m} \tag{19}
$$

190   The horizontal component of eddy viscosity ϵ_y, is left unmodified.

2.5   Wind Turbine Power Calculation

WakeBlaster calculates the power output using power curve input from the user. In order to calculate accurate power, corresponding to the variant wind speed across the rotor, a rotor equivalent wind speed (U_{rot}) is calculated. This is done by first calculating the combined ambient and wake axial velocity ($U = U_{amb}u$ at the rotor plane), and then integrating across the rotor

195   disk area:

$$
U_{rot} = \sqrt[n]{\int_A U^n dA} \tag{20}
$$

where n is an integer. A popular approach is to use $n = 3$, based on the principle that power is proportional to the cube of the wind speed as suggested in IEC61400-12-1 (2017). However, WakeBlaster uses a value of $n = 1$ by default, i.e. a linear average, with validation having shown this to lead to a more accurate prediction of power output. As this method is performed
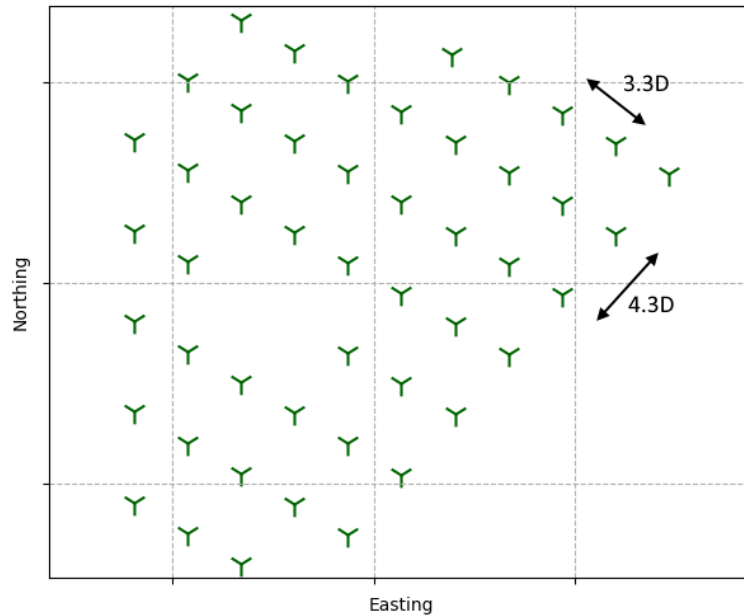
Figure 2. Layout of the Lillgrund wind farm. The turbine rotor diameter is 93 m with a hub height of 68 m. The turbine spacing is approximately 4.3 rotor diameters along the South-West to North-East rows and 3.3 diameters along the South-East to North-West rows.

200 on the combined ambient and wake axial velocity, the effects of wind shear on power production are implicitly included whenever the severity of the wind shear depends on the turbulence and atmospheric stability of the flow case.

  A general directional variability of the wind within each flow case is included in a standard power curve. A rotor yaw angle can be set per turbine, to consider in the power calculation a known average directional misalignment with the rotor plane. A model to modify the power curve for site specific directional variability over the rotor, for example changes with height or for

205 specific meteorological conditions, is not included in the model.

  WakeBlaster uses IEC methods in IEC61400-12-1 (2017) to adjust the power curve for air density and turbulence intensity. The rotor equivalent turbulence intensity is also calculated using the integral method above, but instead using a value of $n = 2$.

3 Simulation Results

In this section we verify the computational performance for large wind farms, and then show the model predictions for an

210 offshore wind farm.

3.1 Computational Performance

WakeBlaster is a medium fidelity tool, which is typically capable of running each flow case in a few seconds, on the single core of a modern processor. With the default settings (a flow plane resolution of 0.1 rotor diameters, and a domain height of three diameters), the time (in seconds) to run a single flow case (T_{fc}) is (on an Intel i5 8$^{\text{th}}$ generation processor) approximately:

215
$$T_{fc} \approx 0.0015 \frac{A}{D^2} \text{ s} \tag{21}$$

where A is the area of the wind farm and D is the rotor diameter. The T_{fc} is proportional to the area of the wind farm, and (at equal turbine density) proportional to the number of wind turbines in the wind farm. However, the exact time will depend on the wind farm's layout, the wind direction and the processor architecture. The T_{fc} is also proportional to the cube of the flow plane resolution, although results do not show any significant improvement in accuracy when the resolution is increased.

220 For example, a typical flow case for Horns Rev runs in about 5 s, and the largest farms in the North Sea under planning around a minute. Unless hysteresis effects are included in a time series simulation, each required flow case remains independent from the others, allowing many flow cases to be run in parallel. As WakeBlaster is hosted on the cloud, this allows a high level of parallelisation across dozens of processors, meaning that an energy assessment consisting of (for example) 2,000 flow cases can be completed in a matter of minutes, even for large wind farms.

225 ### 3.2 Waked Flow Visualisation

As a three-dimensional wake model, it is possible to create plots of the three-dimensional waked flow field for the complete wind farm for a particular flow case. In this article, a visualisation of a single flow case from the Lillgrund wind farm, located in the Øresund Strait, between Sweden and Denmark, is presented. The Lillgrund wind farm presents a good case study, because the small spacing between turbines (3.3 and 4.3 rotor diameters, along the two principal rows) leads to large wake effects. The

230 layout is shown in figure 2.

Three cross-sectional slices in the xy, xz and yz planes, for a flow case of 8 m/s wind speed, 270 deg wind direction and 6 % turbulence intensity, are presented in figure 3.

These simulations indicate that there is significant interaction between the wakes originating from each turbine, and this supports the assumption that the wakes cannot be modelled independently. The wake interaction leads to a complex wind farm

235 wake shape at the downstream end of the farm. The low hub height of the wind turbines (68 m), relative to their rotor diameter (93 m), results in significant ground-wake interaction effects. Due to the fact that ambient mixing from below is limited, single turbine wakes become asymmetrical in shape, and the point of greatest deficit drifts downwards to below hub height.
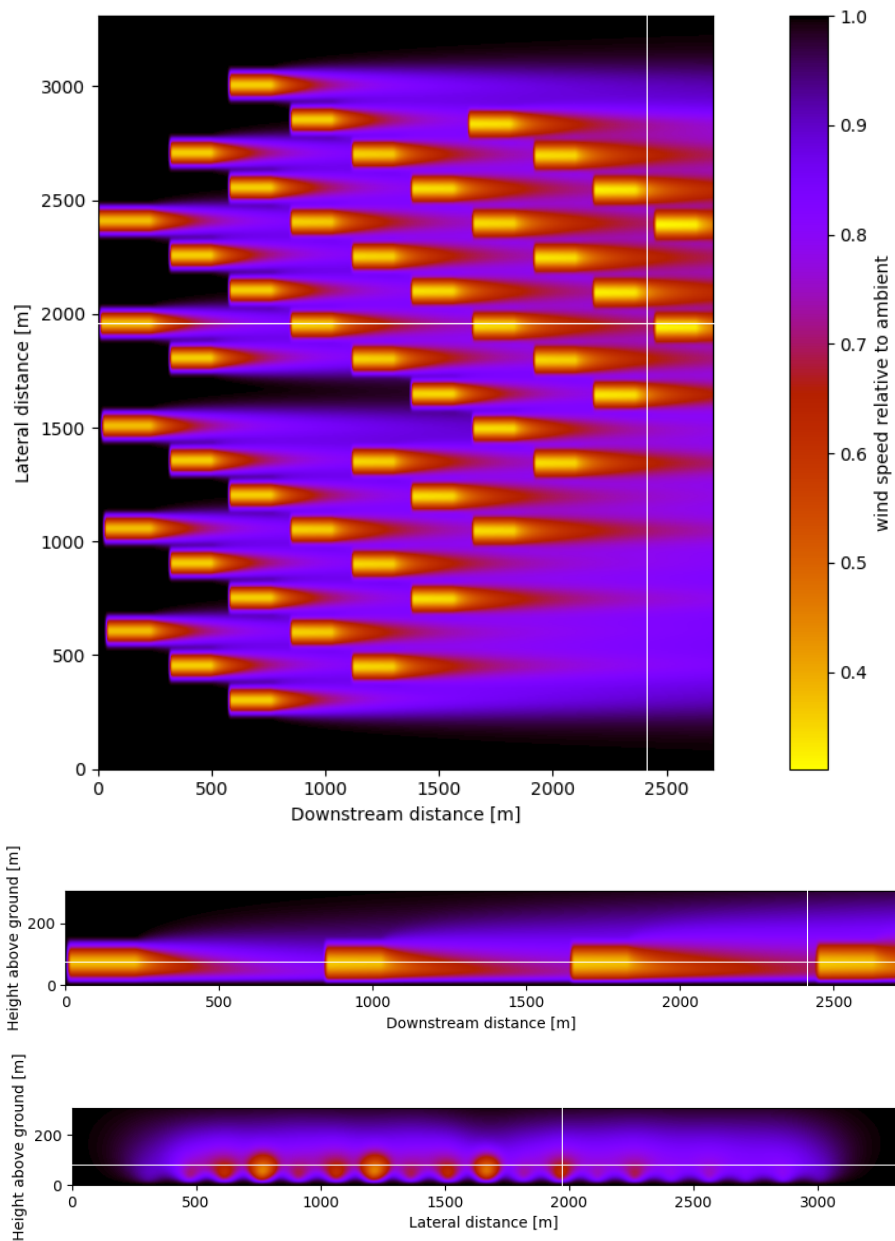
Figure 3. Plots of the axial velocity in the wind farm relative to ambient wind speed for a flow case of 8 m/s with the wind from due West. From top to bottom: xy (birds-eye) slice at hub height; xz (side-on); yz (front-on). The white lines show the corresponding planes of the other plots. The xy plot is taken at the turbine hub-height above sea-level - 68 m.

4 Limitations

The code is a mid-fidelity code designed to be fast and capable of simulating projects with several thousand turbines, working with limited amount of readily available input data and be used in an iterative design process. This limits the level of detail that can be included in the sub-models.

- No direct interaction between the turbines and no description of the axial pressure gradient are included in the model. The induction zones directly upstream and downstream (near wake) of turbines can overlap and interact. This may lead to changes in turbine performance and turbine characteristics and no attempt has been made to quantify such effects.

- A basic representation of the the ambient flow is used as input to the model. The wake is modelled as a perturbation of the underlying flow. No attempt has been made to model a two-way interaction with the atmospheric boundary layer.

- The model is designed for stationary flow cases. No detailed models representing dynamic changes in wind direction, wind speed or turbine control were included.

- The ambient wind direction is assumed to be constant throughout the wind farm. Therefore in curved flows (due to terrain or due to meteorological factors), downstream wake locations may not be accurate.

The WakeBlaster model undergoes continuous, data driven improvement, and refined models will be added successively.

5 Conclusions

This is the first publication to present the theoretical background of WakeBlaster in some detail. WakeBlaster is a recently developed 3D-RANS solver that is specialised to simulate the waked flow field in wind farms. The characteristics of this model show the desired performance balance between speed and realistically achievable accuracy.

The model has been validated against performance data from offshore and onshore wind farms. Further detailed validation will focus on the specific 3D elements of the model, such as wake superposition and wake boundary layer interaction.

Code availability. WakeBlaster calculations are provided as a cloud service and designed for integration in other software packages. Wake-Blaster is available from ProPlanEn directly (www.wakeblaster.net) and through third party implementations. WakeBlaster has been integrated in EMD's WindPro software and is scheduled for release in April 2020.

Author contributions. Philip Bradstock: formal analysis, investigation, methodology, software development, data curation, verification, validation, visualisation, writing; Wolfgang Schlez: conceptualisation, funding acquisition, project administration, resources, investigation, supervision, methodology, writing

Competing interests. The authors declare that they have no conflict of interest.

265   *Acknowledgements.* The development of WakeBlaster was co-funded by the UK's innovation agency, Innovate UK. A number of companies contributed operational wind farm data to this research, and their support is greatly appreciated. ProPlanEn GmbH processed the Lillgrund test case, as part of IEA task-31: WakeBench. The contributions of Staffan Lindahl (validation and visualisation), Michael Tinning (software development) and Vassilis Kostopoulos (validation, investigation, data curation and methodology) are acknowledged.

References

270 Abramovich, G. N.: The Theory Of Turbulent Jets, M.I.T Press, Cambridge, Massachusetts, USA, 1963.

Ainslie, J.: Calculating the Flowfield in the Wake of Wind Turbines, Journal of Wind Energy and Industrial Aerodynamics, 27, 213–224, 1988.

Barthelmie, R., Frandsen, S., Rathmann, O., Hansen, K., Politis, E., Prospathopoulos, J., Schepers, J., Rados, K., Cabezon, D., Schlez, W., Neubert, A., and Heath, M.: Flow and Wakes in Large Wind Farms: Final Report for UPWIND WP8, Tech. Rep. Risø-R-1765 (EN), Risø,
275 2011.

Beaucage, P., Brower, M., Robinson, N., and Alonge, C.: Overview of Six Commercial and Research Wake Models for Large Offshore Wind Farms, in: European Wind Energy Association Conference 2012, 2012.

Burden, R. L. and Faires, J. D.: Numerical Analysis. 2001, Brooks/Cole, USA, 2001.

Businger, J. A.: Transfer of Heat and Momentum in the Atmospheric Boundary Layer, in: Proc. Arctic Heat Budget and Atmospheric
280 Circulation, 1966.

Businger, J. A.: Flux-Profile Relationships in the Atmospheric Surface Layer, Journal of the Atmospheric Sciences, 28, 181–189, 1971.

Crespo, A., Hernandez, J., Fraga, E., and Andreu, C.: Experimental Validation of the UPM Computer Code to Calculate Wind Turbine Wakes and Comparison With Other Models, Journal of Wind Engineering and Industrial Aerodynamics, 27, 77–88, 1988.

Crespo, A., Chacón, L., Hernández, J., Manuel, F., and Grau, J.: UPMPARK: a Parabolic 3D Code to Model Wind Farms, Proceedings of
285 EWEC 1994, pp. 454–459, 1994.

Crespo, A., Hernandez, J., and Frandsen, S.: Survey of Modelling Methods for Wind Turbine Wakes and Wind Farms, Wind energy, 2, 1–24, 1999.

Eecen, P. J., Wagenaar, J. W., and Bot, E. T. G.: Offshore Wind Farms: Losses and Turbulence in Wakes, Tech. Rep. ECN-M–11-065, ECN, 2011.

290 Ferziger, J. H., Peric, M., and Leonard, A.: Computational Methods for Fluid Dynamics, AIP, 1997.

IEC61400-12-1: Wind Turbines:Power Performance Measurement Verification of Electricity Producing Wind Turbines, Standard, International Electrotechnical Commission, 2017.

Ishihara, T. and Qian, G.-W.: A new Gaussian-Based Analytical Wake Model for Wind Turbines Considering Ambient Turbulence Intensities and Thrust Coefficient Effects, Journal of Wind Engineering and Industrial Aerodynamics, 177, 275–292, 2018.

295 Jensen, N.: A Note on Wind Generator Interaction, Tech. Rep. M-2411, Risø National Laboratory, Roskilde, Denmark, 1983.

Laan, M. P., Sørensen, N. N., Réthoré, P.-E., Mann, J., Kelly, M. C., and Troldborg, N.: The k-ϵ-fP Model Applied to Double Wind Turbine Wakes Using Different Actuator Disk Force Methods, Wind Energy, 18, 2223–2240, https://onlinelibrary.wiley.com/doi/abs/10.1002/we.1816, 2017.

Liddell, A., Schlez, W., Neubert, A., Pena, A., and Trujillo, J.: Advanced Wake Model for Closely Spaced Turbines, in: AWEA Denver 2005,
300 2005.

Lissaman, P.: Energy Effectiveness of Arbitrary Arrays of Wind Turbines, AIAA Journal of Energy, New York, 3,6, 1979.

Lissaman, P., Gyatt, G., and Zalay, A.: Numeric-Modelling Sensitivity Analysis of the Performance of Wind-Turbine Arrays, Tech. Rep. UC-60, Aerovironment, Inc, Pasadena, California, USA, 1982.

Martinez-Tossas, L. A.: A Three Dimensional and Extremely Fast Wake Solver with Terrain Features for Wind Farm Control, in: Wind
305 Energy Science Conference, 2019.

Michelsen, J. A.: Block Structured Multigrid Solution of 2D and 3D Elliptic PDE's, Tech. Rep. AFM 94-06, DTU, 1994.

Ott, S.: Linearised CFD Models For Wakes, Tech. Rep. Risoe-R-1772(EN), Danmarks Tekniske Universitet, Risø Nationallaboratoriet for Bæredygtig Energi. Denmark. Forskningscenter Risoe, 2011.

Peaceman, D. and Rachford, H.: The Numerical Solution of Parabolic and Elliptic Differential Equations, J. Soc. Indust. Appl. Math., 3, 310   28–41, 1955.

Porté-Agel, F., Bastankhah, M., and Shamsoddin, S.: Wind-Turbine and Wind-Farm Flows: A Review, Boundary-Layer Meteorology, https://doi.org/10.1007/s10546-019-00473-0, 2019.

Prospathopoulos, J. M., Rados, K. G., Cabezon, D., Schepers, J. G., Politis, E., Hansen, K., Chaviaropoulos, P. K., and Barthelmie, R. J.: Simulation of Wind Farms in Flat and Complex Terrain using CFD, in: Torque 2010: The Science of Making Torque from Wind, pp. 315   359–370, 2010.

Schepers, J.: ENDOW: Validation and improvement of ECN's Wake Model, Tech. Rep. ECN-C-03-034, ECN, 2003.

Schlez, W., Neubert, A., and Smith, G.: New Developments in Precision Wind Farm Modelling, in: DEWEK 2006, 22-23 November 2006, Bremen, Germany, 2006.

Schlez, W., Bradstock, P., Tinning, M., and Lindahl, S.: Virtual Wind Farm Simulation A Closer Look at the WakeBlaster Project, WindTech 320   International, 13, https://www.windtech-international.com/editorial-features/a-closer-look-at-the-wakeblaster-project, 2017.

Thomas, L.: Elliptic Problems in Linear Difference Equations Over a Network, Tech. rep., Waston Sci. Comput. Lab. , Columbia University, New York, USA, 1949.

Trabucchi, D., Vollmer, L., and Kühn, M.: 3-D Shear-Layer Model for the Simulation of Multiple Wind Turbine Wakes: Description and First Assessment, Wind Energy Science, 2, 569, 2017.

325 Vermeer, L., Sørensen, J. N., and Crespo, A.: Wind Turbine Wake Aerodynamics, Progress in Aerospace Sciences, 39, 467–510, 2003.

von Rosenberg, D. U.: Methods for the Numerical Solution of Partial Differential Equations, American Elsevier Publishing Company, Inc., New York, USA, 1983.